Vortex Catchment

Filip Sadlo*, Grzegorz Karch†, Marcel Hlawatsch‡, Daniel Weiskopf§, Thomas Ertl¶
Visualization Research Center (VISUS), University of Stuttgart

ABSTRACT

We introduce vortex catchment as a means for analyzing time-dependent vortex development and vortex dynamics in general. We utilize the Lagrangian frame, providing insight into the spatiotemporal mechanisms that relate to a given vortex region. Thereby, our focus is on a gradual and continuous visualization, meeting the gradual properties of vortices. This is achieved by deriving scalar quantities in space-time projections that allow for visualization by volume rendering. For expressive visualization, we introduce new transfer function strategies for conveying both the spatiotemporal content as well as the underlying dynamics.

Index Terms: vortex dynamics visualization, vorticity transport, time-dependent flow.

1 INTRODUCTION

Vortices play an important role in a wide field of applications. In turbomachinery they are mostly unwanted due to their negative impact on efficiency and lifetime of machines. Examples include reduced throughput, oscillations, and abrasion.

A wide part of the literature is concerned with vortex detection criteria—typically scalar fields—that indicate the presence of a vortex at the respective points in space and time. Examples include the magnitude of *vorticity* $\boldsymbol{\omega} = \nabla \times \boldsymbol{u}$ (curl of velocity $\boldsymbol{u}$), *helicity* $\boldsymbol{\omega} \cdot \boldsymbol{u}$, Q [4], Δ [1], and λ_2 introduced by Jeong and Hussain [5]. Despite those pointwise approaches, concepts have been proposed that employ a Lagrangian scope, i.e., conduct analysis relative to moving particles [2, 3]. The present work can be seen as an extension of our previous work [7] on vorticity transport. We now provide a continuous approach for analyzing the spacetime (catchment) regions that contribute to a vortex.

2 VORTEX CATCHMENT

In our work on the visualization of vortex dynamics in time-dependent flow [7] we visualized the mechanisms that lead to a given vortex by integrating path lines in upstream direction starting at its vortex core line. Mapping vorticity to the thickness of the path line tube and adding vorticity streamlets seeded regularly along the tube conveys the directional configuration of velocity and vorticity as well as vorticity magnitude. Further effects such as vortex stretching and tilting were color coded on the path line tubes.

This approach takes into account that vorticity is usually generated in wall shear layers and then transported by advection and diffusion to the vortex regions, forming vortex catchment regions. On its way, the most important mechanism is tilting of the vorticity vector relative to velocity—between its orthogonal configuration in shear flow, and parallel configuration in vortices. Related to helicity, we call this angle *helicity angle*.

*e-mail: sadlo@visus.uni-stuttgart.de
†e-mail: grzegorz.karch@visus.uni-stuttgart.de
‡e-mail: marcel.hlawatsch@visus.uni-stuttgart.de
§e-mail: weiskopf@visus.uni-stuttgart.de
¶e-mail: thomas.ertl@vis.uni-stuttgart.de

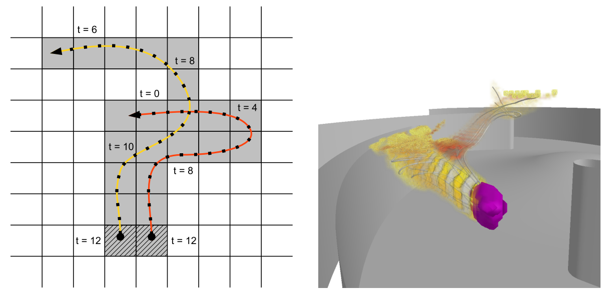

(a) (b)

Figure 1: (a) Spatiotemporal analysis of vortex catchment. For each voxel (hatched squares) of the vortex region (time $t_0 = 12$), path lines (red and yellow lines) are traced in upstream direction (backward in time). Physical properties are sampled along these path lines (black dots) and stored in a regular grid (grey squares). Every cell can be visited multiple times for different points in time, e.g., when different path lines traverse the same cell. Therefore, the cells store spatiotemporally averaged values of the properties. (b) Visualization of vortex catchment dynamics with additional animated "time stripes" (modulation of saturation) to convey flow into vortex region (purple).

Our previous approach [7] is discrete, in the sense that it builds on vortex core line features and visualizes individual path lines started from them. In our new approach, we aim at a gradual and continuous visualization. Let vorticity magnitude map to opacity of the path lines and the helicity angle to color. Our new approach can be identified as the limit case with infinite line density: vorticity magnitude and helicity angle are both sampled along path lines and projected on a spatial sampling grid with subsequent volume rendering. To take the continuous nature of vortices further into account, the path lines are seeded from volumetric regions instead of core lines. In our approach we applied a thresholding of the λ_2 field to define those regions (Section 2.1).

2.1 Identification of Instantaneous Vortices

Our vortex catchment visualization technique is based on target regions representing vortices, called *vortex regions*. These regions subsequently serve as seeds for our path line based analysis technique (Section 2.2). In our approach the vortex regions are obtained by imposing a threshold τ on a vortex criterion, i.e., selecting the set of points where the criterion passes the threshold. Any vortex criterion would be applicable, we have chosen the λ_2 criterion for its wide use in science and engineering. The threshold τ is manually chosen, supported by browsing through time-dependent data.

To reduce occlusion and clutter, we select vortex regions by interactive picking and extract them by connected component labeling. As described in Section 2.4 we compute the criteria on the original (unstructured) grid but use a resampled version for the filtering by connected component labeling and projection (Section 2.2).

2.2 Analysis of Catchment

Having the individual vortex regions at time t_0 discretized on a regular grid (Section 2.1), we analyze the flow mechanisms that lead to each vortex region. This is achieved by starting path lines from the selected region at t_0 (Fig. 1 (a)) in upstream direction (backward in time). Along these path lines, we sample vorticity magnitude and the helicity angle at the respective points in space and time, and additionally the integration time at which the path line particle passed this location. These quantities are accumulated inside our uniform sampling grid, which represents a temporal projection to time t_0. This results in a 3D data set for t_0 and can be repeated for each time step of the data. Each data set depicts the dynamics in terms of vorticity transport with respect to the respective t_0.

Since path lines typically diverge over time, starting one path line from each voxel inside a vortex region is not sufficient to obtain a dense sampling. This is accounted for by supersampling, i.e., by starting multiple path lines from each voxel, which can be done in a progressive manner for fast preview generation. The obtained data lends itself to visualization by volume rendering (see Section 3).

2.3 Tracking

If the vortex catchment analysis is required for multiple steps of time-dependent data, e.g., for computing a movie, the selected vortex region is tracked and the steps from Section 2.1 and Section 2.2 are repeated for each step. We track the vortex region using a simple approach: we compute the center of gravity of this region and use it as selection point for the next step. If no object is hit, we use the object voxel closest to the center of gravity. The tracking is done in reverse time, starting with the latest time step. This is because in the beginning, vortices are often not well developed and close to walls, hence identification and selection would be difficult

This simple approach can fail with non-convex objects or if the object is moving too fast compared to the time discretization. Furthermore, it does not address split/merge events. However, it turned out that this approach worked well enough in our experiments. Because we focus on vortex dynamics, and because our vortex catchment already provides continuity in spacetime, we address inclusion of more sophisticated tracking techniques as future work.

2.4 Technical Details

The data for the final visualization by volume rendering is stored on a static, regular sampling grid. However, the computation of quantities, such as λ_2, and path line integration are performed on the original grid. In the case of rotating grid geometry, all quantities are computed from velocity in stationary frame to avoid deviation due to superimposed rotation of the velocity field. Integration is done using the fourth order Runge-Kutta scheme with adaptive step size control. Gradients are computed using least squares fitting.

3 Visualization Environment and Workflow

Our visualization environment consists of two independent applications. We use the modular visualization framework AVS [8] for pre-processing of the data, which took in our experiments about 2 minutes per time step (t_0). For interactive visualization of the final result, we developed a standalone CUDA-based volume renderer, which employs ray casting.

We used the following workflow to obtain our result: the dataset is loaded in AVS using our own CFX reader module. The data is then dumped in spacetime coherent order for efficient access using *mmap* [6]. First, a region of interest is defined, where the vortex analysis is performed. For this, the λ_2 criterion is computed and isosurfaces of the resulting field are visualized. After selecting a suitable region of interest, the vortex catchment is computed. The resulting scalar fields and geometries for path lines and isosurfaces are saved to disk. This data is loaded at run time in the interactive volume rendering application. An interactively adjustable transfer function is used with separated channels for color and opacity. This transfer function maps helicity angle to color and vorticity magnitude to opacity (see Figure 2). Further, we provide time-dependent transfer function modulation to visualize the transport

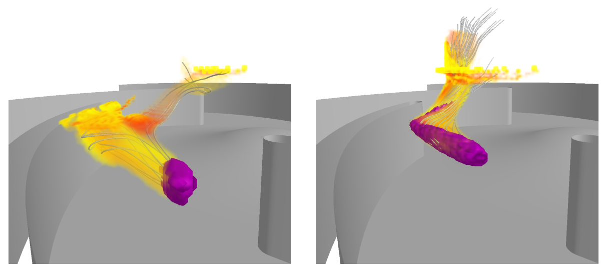

(a) (b)

Figure 2: Visualization of vortex catchment. The purple surface represents vortex region. Volume rendering is used to visualize helicity angle as color, and vorticity magnitude as opacity. Yellow color denotes shear flow (high angle) and red color indicates vortical flow (low angle). Two vortices are depicted: one has its source at the wall and its creation is dominated by shear flow (a); the other evolves from the top (where fluid flows in) and develops from both shear flow and vortical flow (b).

(Figure 1 (b)). This function simply visualizes the sampled trajectory time using a shifting box function sequence.

4 Conclusion and Future Work

Our technique reveals the mechanisms behind time-dependent vortical flow. In particular, it gives insight where vorticity is obtained from, how it changes its role from shear flow to vortical flow on its way through spacetime into vortices, and how vortices and shear flow interact. In the case of the data from the centrifugal pump simulation, our method visualizes not only which stall cells are in relation with vortices, but also their interplay.

Acknowledgements

The authors would like to thank the German Research Foundation (DFG) for financial support of the project within the *Cluster of Excellence in Simulation Technology* (EXC 310/1) and the Collaborative Research Centre SFB-TRR 75 at Universität Stuttgart.

References

[1] M. Chong, A. Perry, and B. Cantwell. A general classification of three-dimensional flow fields. *Phys. Fluids*, A 2(5):765–777, 1990.

[2] R. Cucitore, M. Quadrio, and A. Baron. On the effectiveness and limitations of local criteria for the identification of a vortex. *European Journal of Mechanics - B/Fluids*, 18(2):261 – 282, 1999.

[3] R. Fuchs, R. Peikert, F. Sadlo, B. Alsallakh, and M. E. Gröller. Delocalized unsteady vortex region detectors. In D. S. Oliver Deussen, Daniel Keim, editor, *Proceedings VMV 2008*, pages 81–90, Oct. 2008.

[4] J. Hunt, A. Wray, and P. Moin. Eddies, stream, and convergence zones in turbulent flows. Technical Report CTR-S88, Center for Turbulence Research, NASA Ames Research Center and Stanford University, 1988.

[5] J. Jeong and F. Hussain. On the identification of a vortex. *Journal of Fluid Mechanics*, 285(69):69–94, 1995.

[6] F. Sadlo and R. Peikert. Efficient visualization of lagrangian coherent structures by filtered amr ridge extraction. *IEEE Trans. Vis. Comput. Graph.*, 13(6):1456–1463, 2007.

[7] F. Sadlo, R. Peikert, and M. Sick. Visualization tools for vorticity transport analysis in incompressible flow. *IEEE Trans. Vis. Comput. Graph.*, 12(5):949–956, 2006.

[8] C. Upson, T. Faulhaber JR, D. Kamins, D. Laidlaw, D. Schlegel, J. Vroom, R. Gurwitz, and A. Van Dam. The application visualization system: A computational environment for scientific visualization. *IEEE Computer Graphics and Applications*, 9(4):30–42, 1989.

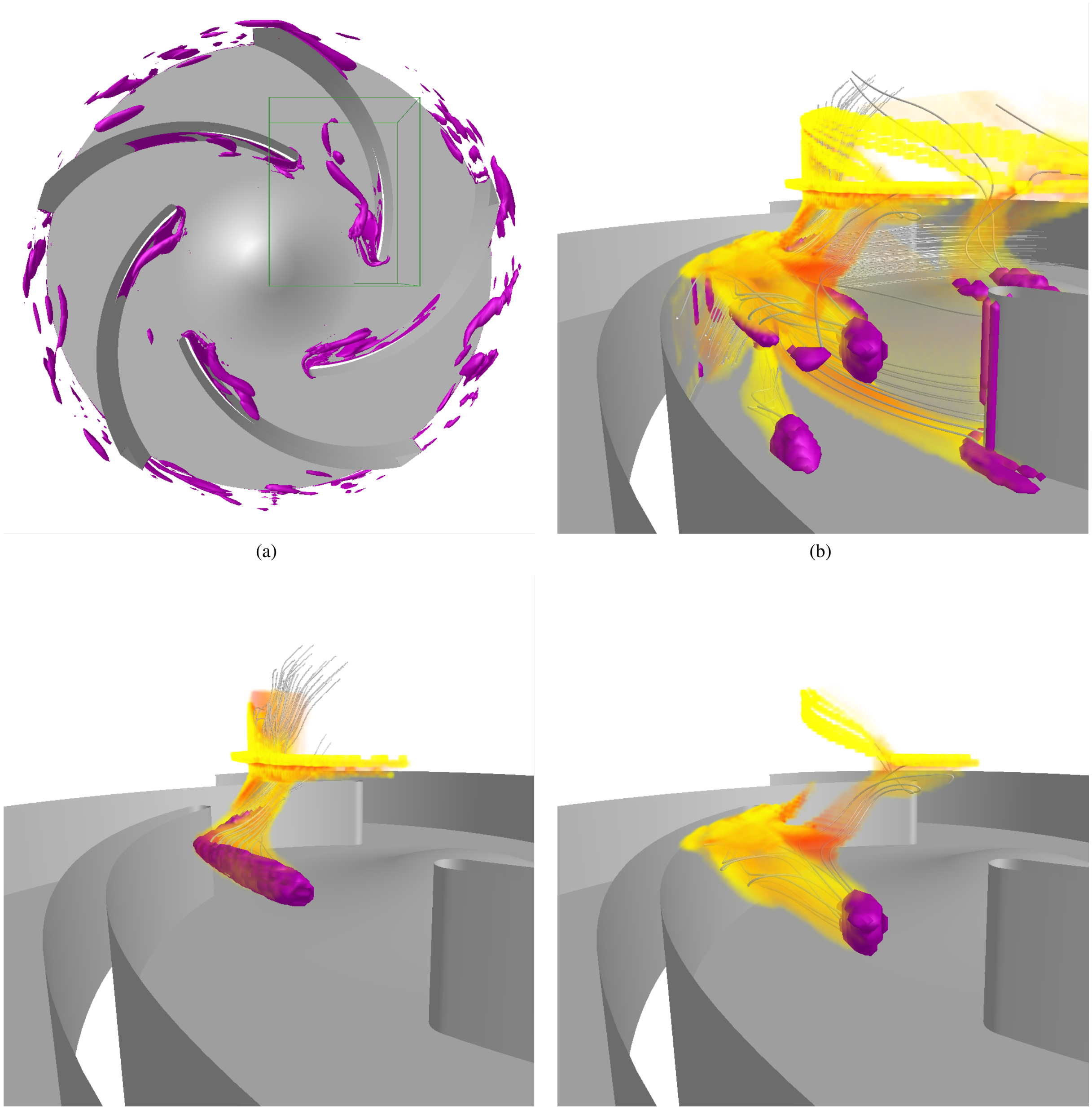

(a) (b)

(c) (d)

Figure 3: Detailed analysis of vortex catchment at impeller blade. (We omit the downstream part of the pump from the analysis due to absent inflow into the runner from that part and comparably low viscosity, leading to negligible influence in terms of vorticity transport.) (a) Overview of the impeller with the thresholded λ_2 field (purple isosurfaces from unstructured grid) representing vortex regions at $t_0 = 0.873$ seconds and region of interest (green box) (for all results). All remaining isosurfaces are from resampled λ_2. These vortex regions are candidates for the vortex catchment analysis. (We did not evaluate the λ_2 criterion close to the upper wall of the runner to provide better overview.) (b) When visualizing the vortex catchment for all vortex regions, not only occlusion problems occur but also, due to spacetime superposition of multiple catchment regions, the volume rendering exhibits ambiguities. Some of the upstream path lines (advection time -0.04 seconds) are visualized by tubes. To avoid these problems, single vortices are selected. (c) This vortex obtains its vorticity from the inlet of the pump and its catchment is characterized by combined shear (yellow) and vortical (orange) flow. (d) The main source of the second vortex is shear from the blade.

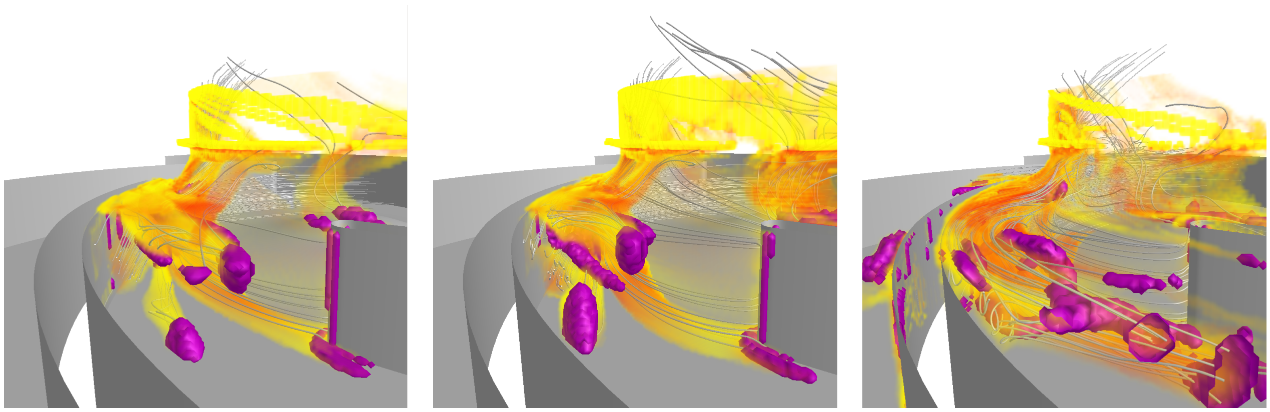

(a) (b) (c)

Figure 4: Visualization of multiple vortex regions for the three turbulence models. (a) shows the result for the DES model, (b) was created with the SST model, and (c) with SAS. As the images show, similar vortical structures and catchment behavior are generated by DES and SST turbulence models but SAS deviates substantially.

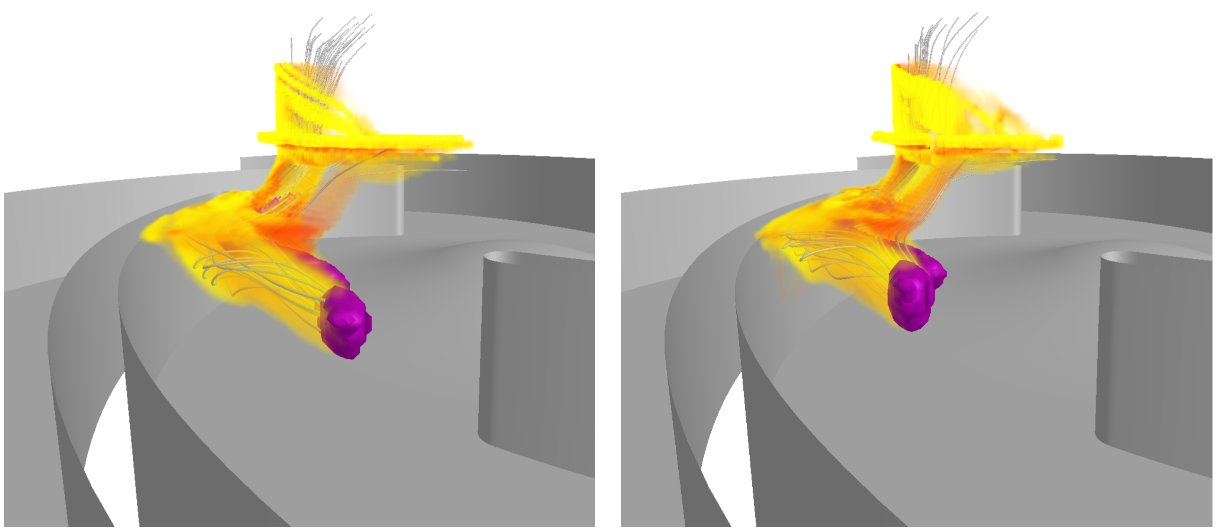

(a) (b)

Figure 5: Visualization of selected analogous vortex regions from DES and SST simulations. Although the catchment is similar, the SST version obtains more vorticity (visible by higher opacity) from the front upper region.

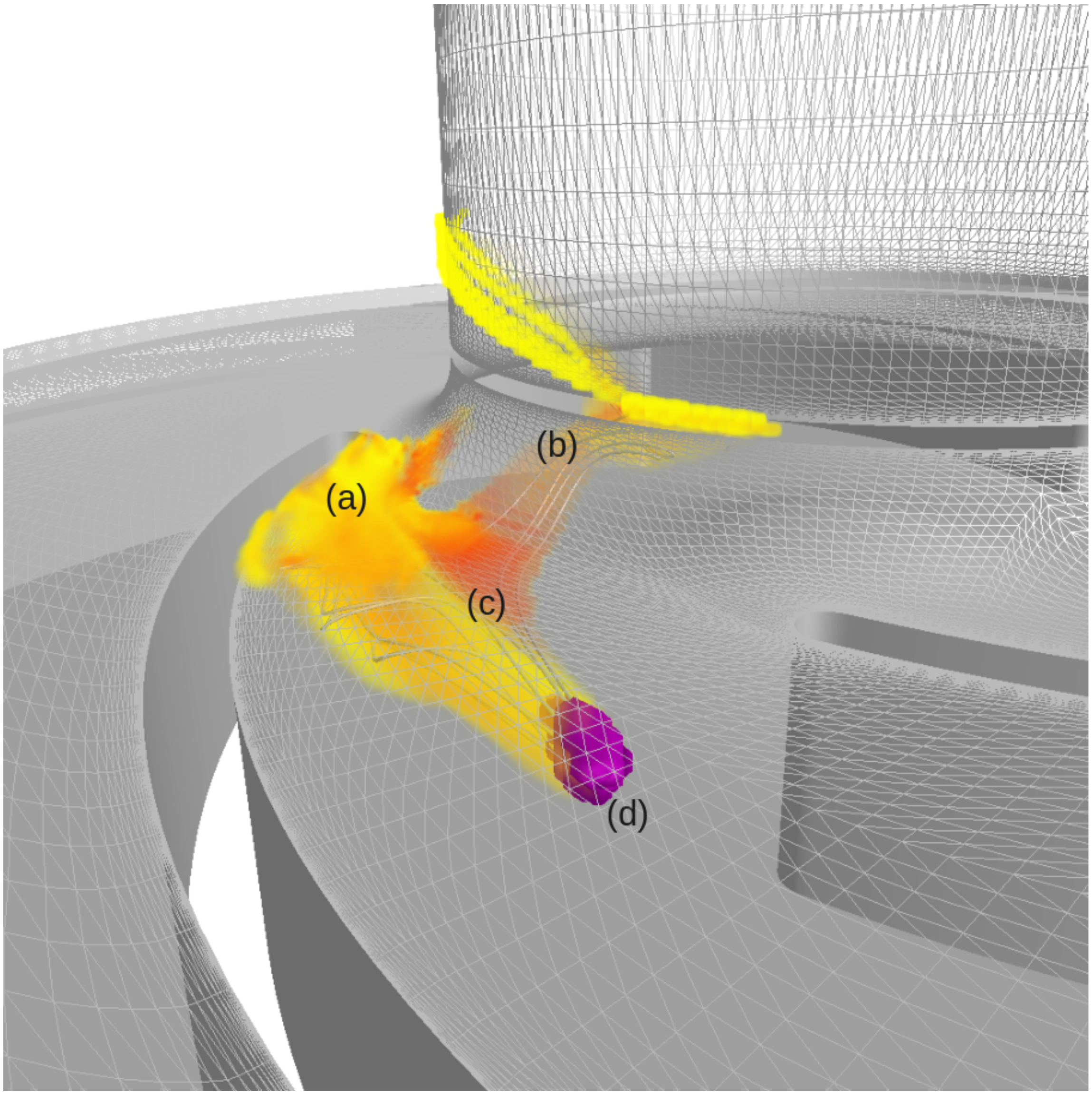

Figure 6: Vortex catchment in DES simulation. The main source of vorticity for this selected vortex region (purple) is the shear flow at the blade (a). Another contribution is from the inlet region (b) where the flow rapidly transforms into vortical flow (orange color) and merges with the shear flow at (c). One can see that part of the catchment area extends to the upper side of the wall (wireframe) through the gap in the geometry at (b).